IEEE Photonics Journal
An IEEE Photonics Society Publication

Fixed Dual-Thickness Terahertz Liquid Spectroscopy Using a Spinning Sample Technique

Volume 1, Number 2, August 2009

Jegathisvaran Balakrishnan, Student Member, IEEE
Bernd M. Fischer
Derek Abbott, Fellow, IEEE

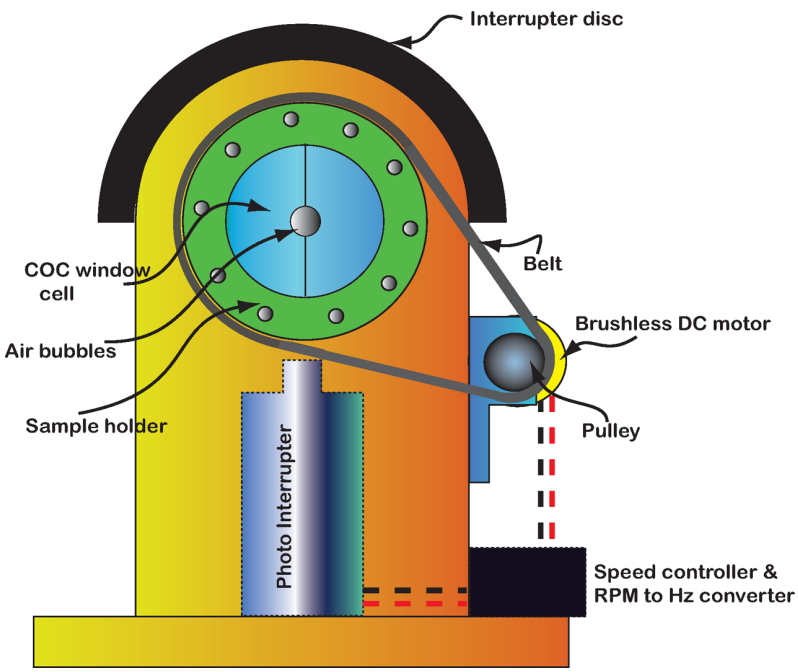

DOI: 10.1109/JPHOT.2009.2027135
1943-0655/$26.00 ©2009 IEEE

Fixed Dual-Thickness Terahertz Liquid Spectroscopy Using a Spinning Sample Technique

Jegathisvaran Balakrishnan,[1] ***Student Member, IEEE,*** **Bernd M. Fischer,**[1,2] **and Derek Abbott,**[1] ***Fellow, IEEE***

[1]Centre for Biomedical Engineering and School of Electrical and Electronic Engineering, The University of Adelaide, Adelaide 5005, Australia
[2]Division IV, ERG, French-German Research Institute of Saint Louis (ISL), 68301 Saint Louis Cedex, France

DOI: 10.1109/JPHOT.2009.2027135
1943-0655/$26.00 ©2009 IEEE

Manuscript received May 22, 2009; revised July 1, 2009. First published Online July 7, 2009. Current version published July 22, 2009. Corresponding author: J. Balakrishnan (e-mail: jega@eleceng.adelaide.edu.au).

Abstract: The conventional double-modulated terahertz differential time-domain spectroscopy (double-modulated THz-DTDS) of liquids requires linear dithering of the sample to rapidly vary the sample thickness in order to produce the required sample and reference signals. Linear dithering, however, imposes a fundamental limitation as it introduces mechanical noise into the system, thereby contributing to measurement uncertainty. In this paper, we address this limitation for the terahertz spectroscopy of liquids by using a fixed dual-thickness sample mounted on a spinning wheel. The concept of spinning the sample allows rapid switching between two fixed sample thicknesses in order to produce sample and reference signals without the introduction of added mechanical noise. We validate this new technique by measuring the dielectric properties of a number of liquids and confirm the results against the Debye relaxation model.

Index Terms: T-rays, terahertz, double-modulated DTDS, differential time-domain spectroscopy.

1. Introduction

Spectroscopic studies on liquid in the terahertz (T-ray) regime have been a topic of interest in recent years. Terahertz liquid spectroscopy allows an analysis of chemical composition and provides a better understanding of the solvation dynamics of various types of liquids. A number of significant studies have motivated the need for terahertz spectroscopy of liquids, including: spectroscopy of biomolecules in aqueous solutions [1], spectroscopy of inflammables in beverage plastic bottles [2], spectroscopy of polar and nonpolar liquids [3]–[6]. Although it has been shown that liquid spectroscopy using T-rays is feasible, the absorption coefficient for liquid water shows a very high terahertz absorption, 200 cm^{-1} at 1 THz [4], [6]. Recently, many measurement techniques have been introduced to improve the sensitivity of terahertz liquid measurement. Hirori *et al.* [7] implemented attenuated total reflection spectroscopy (TD-ATR) for highly absorbing materials such as polar liquids and biomolecules in aqueous solution. Interaction between the sample and the evanescent wave propagating along a prism can be detected via the TD-ATR measurement technique. Also, Cheng *et al.* [8] demonstrated liquid measurements using the evanescent field of a silicon waveguide. In their work, the optical properties of a liquid are obtained based on the interaction between the evanescent wave of a cylindrical silicon waveguide and the liquid sample.

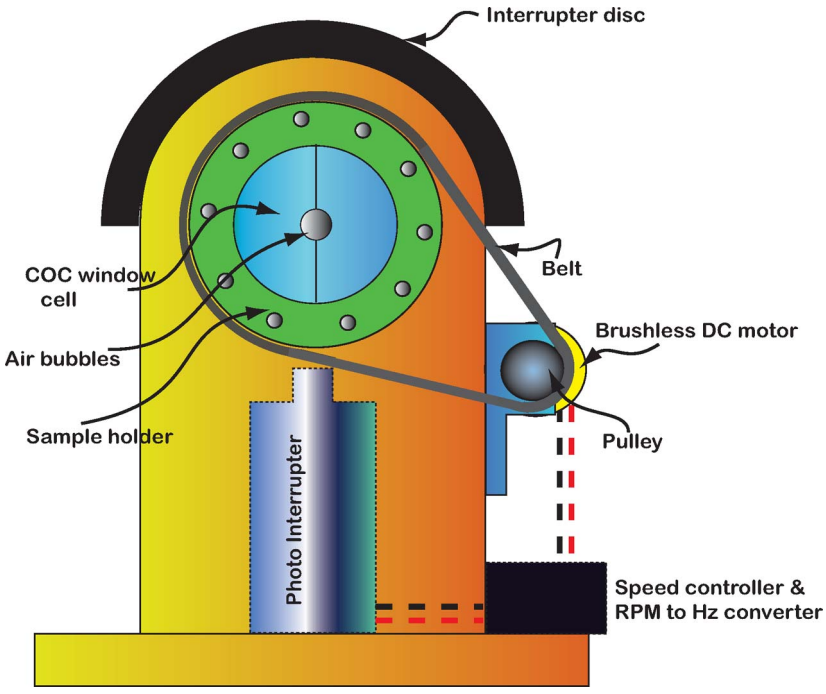

Fig. 1. Spinning wheel for double-modulated DTDS dual-thickness liquid measurement. This figure shows a prototype of the spinning wheel sample holder for a dual-thickness liquid measurement. The wheel is located in the focal plane with a speed setting of 70 Hz. Here, a rapid succession measurement can be achieved as the terahertz beam transmits through the rotating sample. Due to the buoyancy effect, any excess air bubbles present in the liquid sample are desirably pushed to the center of the window cell as the wheel spins [10].

Moreover, implementation of simultaneous measurement of the reference and sample signals using two separate pyroelectric sensors is introduced by Cheng *et al.* In another study conducted by Mickan *et al.* [9], a linear liquid dithering technique using a double-modulated differential time-domain spectroscopy (double-modulated DTDS) has been explored. The linear dithering technique used here allows a dual-thickness measurement where the reference and sample signals are detected through a thick and a thin version of the same liquid. Furthermore, a simultaneous dual-waveform acquisition, resulting in mean and amplitude signals, is achieved by this technique. Although dithering has been demonstrated, inaccuracies in the dual-thickness measurement introduced by the mechanical instability of the dithering mechanism is significantly large. Also, the presence of Fabry–Pérot reflections, due to the very thin sample cell, limits the dithering performance. Furthermore, the presence of macroscopic and microscopic bubbles in a liquid can hinder the accuracy of the measurements.

In this paper, we demonstrate a spinning wheel technique to address the limitation imposed by conventional linear dithering. By mounting a fixed dual-thickness sample on a spinning wheel, we remove the uncertainty introduced by linear dithering. As will be shown in Section 2, this technique has added advantage of allowing a quick succession of measurements between sample and reference. Furthermore, by spinning a liquid sample the bubbles migrate toward the spin axis thereby managing the problem of bubble-induced inhomogeneity in the liquid.

2. Spinning Wheel

Fig. 1 shows the spinning wheel prototype for a fixed dual-thickness terahertz liquid measurement. A spinning wheel is a robust and reliable mechanical device implemented to address the limitation of the linear dithering of the sample. Here, the optical characteristics of liquids are determined using a dual-thickness geometry presented by Mickan *et al.* [9]. However, in that paper, a polyethylene bag,

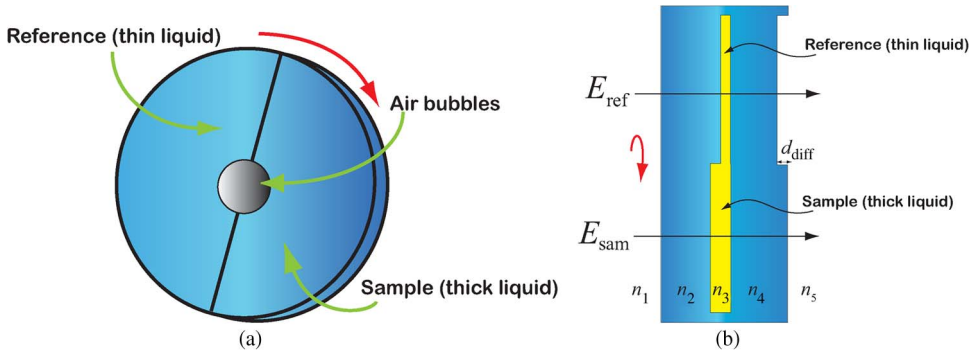

Fig. 2. Fixed dual-thickness geometry of COC 5013L10 window cell. This figure illustrates a fixed dual-thickness sample cell made from COC 5013L10 for a double-modulated DTDS liquid measurement. In (a), the front view of sample holder is shown. The sample holder is designed to be half reference and half sample and mounted onto the spinning wheel as shown in Fig. 1. (b) depicts the cross-sectional view. The window cell has a cavity with two different thicknesses. The reference (thin liquid) is set at 20 μm and the sample (thick liquid) is set at 170 μm. Here, n_1 and n_5 are the refractive index of air, n_2 and n_4 are the refractive index of the COC 5013L10 window cell, and n_1 is the refractive index of the liquid sample under test. Also, d_{diff} is the thickness difference between thin and thick liquid samples.

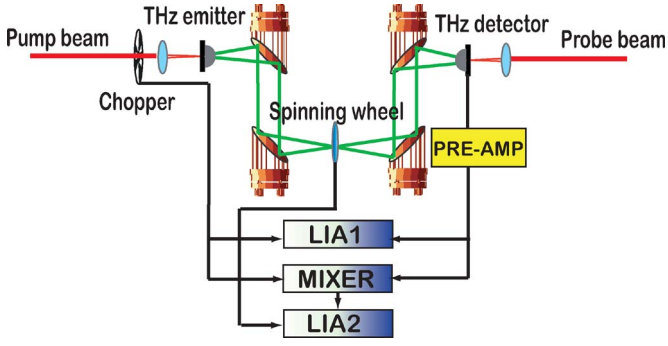

Fig. 3. A double-modulated DTDS spectrometer schematic for dual-thickness liquid measurement. This schematic diagram shows a double-modulated DTDS spectrometer configured for characterizing dielectric properties of liquid samples using a spinning wheel technique. The sample under test is located in the focal plane and modulated at frequency, f_{wheel} of 70 Hz.

which is susceptible to Fabry–Pérot reflections is used as a window material to hold the liquid sample. The dual-thickness measurement was achieved using an audio speaker to dither the liquid sample, leading to an estimated sample thickness error of approximately 100 μm. In this paper, the dual-thickness geometry is achieved by using a fixed thick layer and a fixed thin layer of the same liquid. As the spinning wheel is designed for a transmission experimental setup, the fixed dual-thickness geometry is implemented using a window material known as (TOPAS) cyclic-olefin copolymer (COC) 5013L10. This is because COC 5013L10 is optically transparent, high in transmission and has a low hygroscopicity [11], which makes it ideal for a terahertz liquid spectroscopy. With careful design consideration and molding procedures, the error present in the fixed dual-thickness geometry (Fig. 2) is reduced to less than 5 μm (Fig. 10). Furthermore, this technique has an additional advantage of allowing bubble-free measurements. The bubbles present in the liquid are pushed to the center of the window cell as the wheel spins.

3. Experimental Configuration

The experimental setup for a fixed dual-thickness terahertz liquid measurement using a spinning wheel is shown schematically in Fig. 3. A Mira-SEED Ti-sapphire femtosecond mode-locked laser

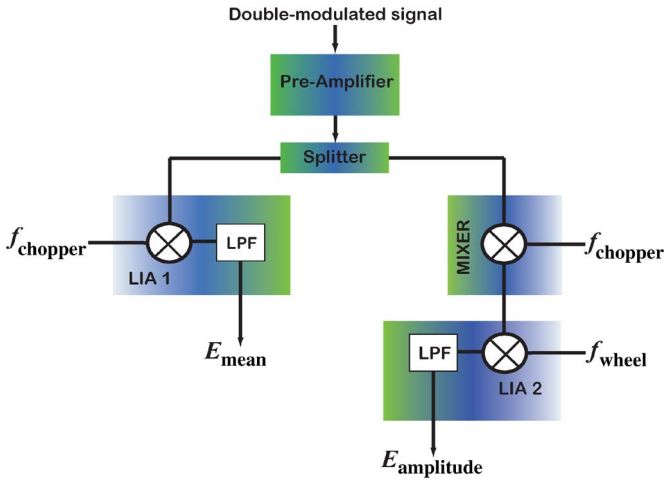

Fig. 4. Lock-in amplifier settings for mean and amplitude signal extraction. In this figure, simultaneous dual-waveform acquisition (mean and amplitude) using two SR830 lock-in amplifiers and a MC1495P mixer is illustrated.

is used to drive the terahertz system. The femtosecond laser produces an output pulse duration of 20 fs at a repetition rate of 76 MHz. This laser generates an output power of 1 W with a center wavelength of 800 nm. The pump beam is modulated at optical chopper frequency, $f_{chopper}$ of 2 kHz. The terahertz pulse is generated due to the modulated pump beam incident on an emitting photoconductive antenna. The terahertz pulse is then collimated and focused onto the rotating dual-thickness liquid sample using the first pair of off-axis parabolic mirrors. The sample under test is located in the focal plane and modulated at frequency, f_{wheel} of 70 Hz. The transmitted terahertz pulse is recollimated and refocused onto the detector using the second pair of off-axis parabolic mirrors. The probe beam gates the incoming transmitted terahertz pulse by focusing the probe laser beam onto the photoconductive antenna at a detector. The detected double-modulated terahertz signal is extracted based on a lock-in amplifier configuration described in the following section.

3.1. Lock-In Amplifier Setting

A double-modulated signal detected at the output of the terahertz system is preamplified using a SR560 preamplifier. The amplified signal is then split by a ZFRSC-2050+ two-way power splitter. One end of the splitter output is connected to the input channel of lock-in amplifier one (LIA1) and the other end of the splitter output is connected to the mixer signal input channel. LIA1 demodulates the incoming terahertz signal with chopper reference signal, $f_{chopper}$, which is then low-pass filtered to produce a mean output signal. The mixer multiplies the incoming signal with the chopper reference signal, $f_{chopper}$, to produce sum and difference components, however, no filtering is applied in the mixer. Thus, the multiplied output of the mixer is then fed into the input channel of lock-in amplifier two (LIA2). Here, LIA2 demodulates the signal detected at the input channel with the spinning wheel reference frequency, f_{wheel}. The demodulated signal is low-pass filtered to produce an amplitude output signal. The lock-in amplifier settings for mean and amplitude signal extraction are illustrated in Fig. 4.

3.2. Sample Preparation

The spinning wheel with a dual-thickness window cell is prepared according to Fig. 1. The thickness of the thin and thick cavities in the window cell is set to 20 μm and 170 μm, respectively (Fig. 2). Here, the window cell thickness is set to 3 mm, which is sufficiently thick to avoid the Fabry–Pérot reflections. Liquid is injected into the cavities through the center hole of the window

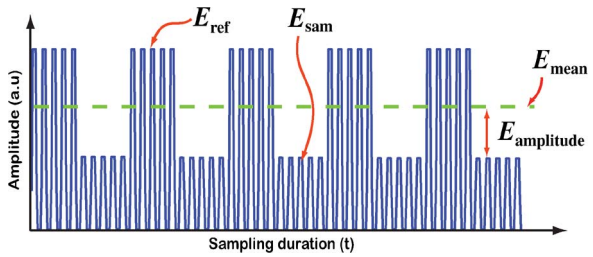

Fig. 5. Modeled output signal of a mixer at nth step of the delay stage. This figure presents a simulated time-domain output signal detected at nth step of the delay stage. The signal is double modulated at $f_{chopper}$ of 2 kHz and f_{wheel} of 70 Hz. The time-domain waveform consists of reference signal, $E_{ref}(t)$, sample signal, $E_{sam}(t)$, mean signal, $E_{mean}(t)$, and amplitude signal, $E_{amplitude}(t)$. Based on the lock-in amplifier settings described in Section 3.1, the $E_{mean}(t)$ and $E_{amplitude}(t)$ are detected at the output channels of LIA1 and LIA2, which are then used to obtain the $E_{ref}(t)$ and $E_{sam}(t)$ signals from the formulas given in Eqs. (1) and (2) [10].

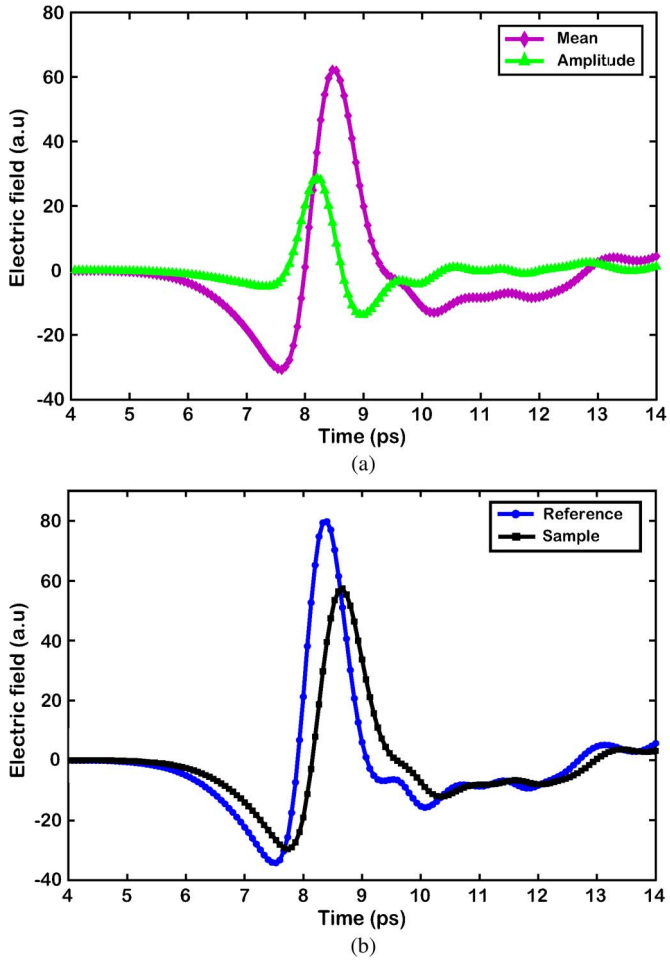

Fig. 6. Time traces of a double-modulated dual-thickness liquid spectroscopy. This figure illustrates typical time profiles of double-modulated dual-thickness liquid measurements. (a) presents the mean and amplitude signals detected at the output channels of LIA1 and LIA2. The mean and amplitude information is then used to plot the reference and sample signals shown in (b) according to Eqs. (1) and (2).

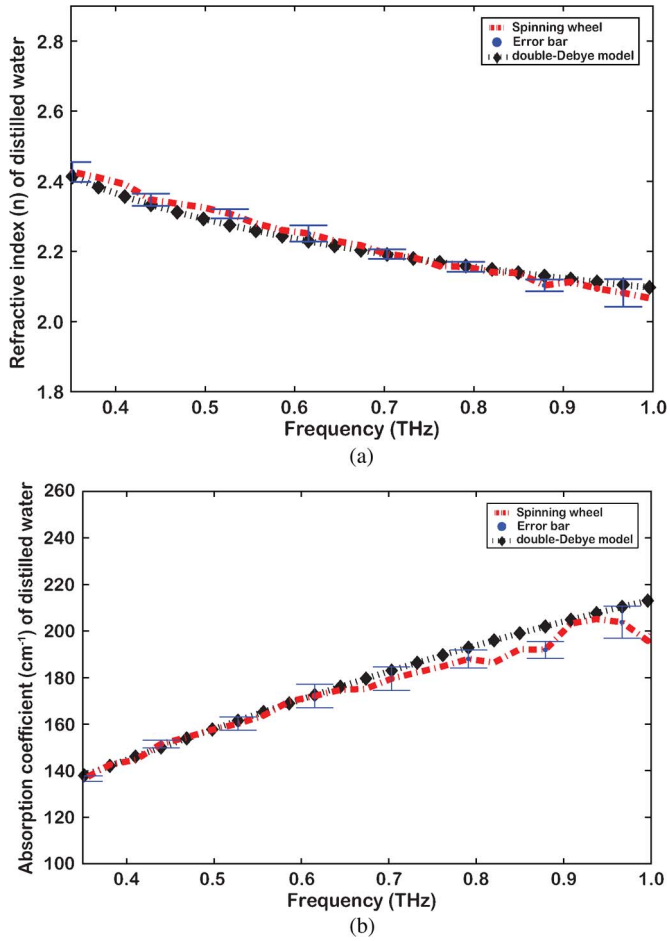

Fig. 7. Refractive index and absorption coefficient of distilled water. This figure compares the experimental results with the double-Debye relaxation model. A good agreement between the measured data and relaxation model is seen. The double-Debye relaxation model is plotted based on the parameters given in [4]. The error bars indicate an estimated uncertainty in the calculated values.

cell using a syringe. In order to increase the signal-to-noise ratio of the measurements, five average scans at a lock-in amplifier time constant setting of 100 ms are used. Moreover, the ambient water vapor spectral lines are reduced by conducting the measurements in a nitrogen-purged environment. The excess liquid present on the surface of the window cell is removed before the measurement. All measurements are conducted at room temperature.

4. Results and Discussion

In this section, we validate the dual-thickness liquid measurement technique using the following liquids: water, methanol, and ethanol. Fig. 5 displays the time-domain waveform detected at *n*th step of the delay stage. The relationships between the reference, $E_{\text{ref}}(t)$, sample, $E_{\text{sam}}(t)$, mean, $E_{\text{mean}}(t)$, and amplitude, $E_{\text{amplitude}}(t)$ signals are presented. Fig. 6 shows typical time profiles for a double-modulated DTDS dual-thickness liquid measurement. In Fig. 6(a), the mean signal detected at the output channel of LIA1 and the amplitude signal detected at the output channel of LIA2 are depicted. Fig. 6(b) illustrates the reference and sample signals obtained based on the extracted mean and amplitude signals. The formulas given in Eqs. (1) and (2) are used to calculate the reference and sample signals. Figs. 7–9 display the terahertz dielectric properties of water,

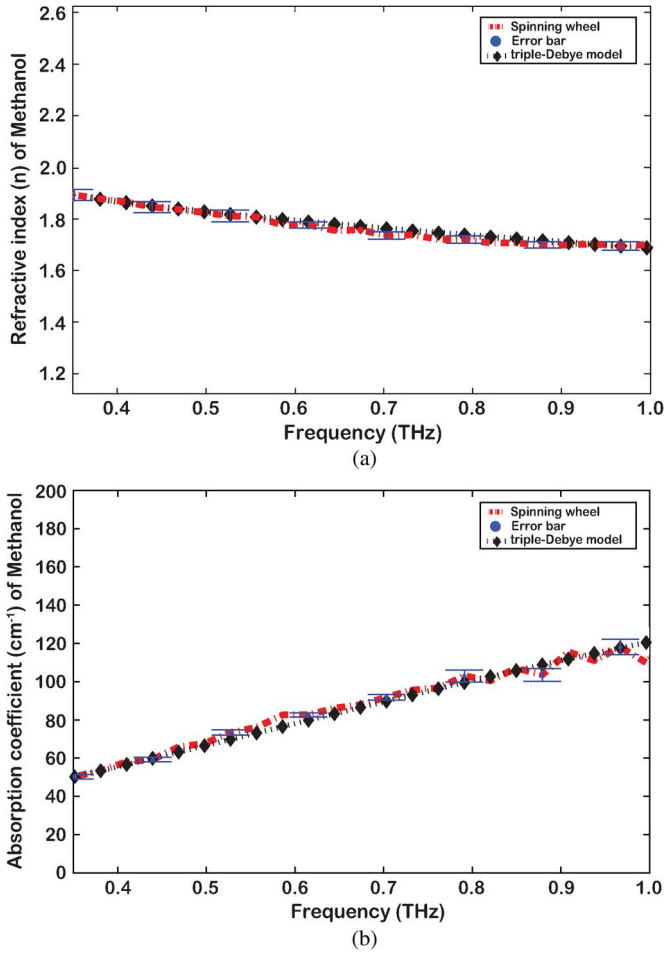

Fig. 8. Refractive index and absorption coefficient of methanol. This figure compares the measured terahertz dielectric properties of methanol with the triple-Debye relaxation model described in the Appendix. The fitting parameters for triple-Debye relaxation model are obtained from [4]. The measured results are in an excellent agreement with the triple-Debye relaxation model reported by [4]. Error bars indicate the amount of uncertainty present in the calculated values.

methanol, and ethanol. The accuracy of the measurement results is compared with the Debye relaxation model.

4.1. Water

Water is known to have high absorption in the terahertz frequency band, typically 200 cm^{-1} at 1 THz [4]. For the past decades, many studies have been conducted to analyze the dielectric response of liquid water in the terahertz frequency range. The dielectric response provides valuable information on solvation dynamics of liquid. In this paper, an alternative measurement using a double-modulated dual-thickness spinning wheel technique to measure the dielectric properties of liquid water is shown. Fig. 7 illustrates the refractive index and the absorption coefficient of liquid water. According to Fig. 7(a), close match can be seen between the measured refractive index and the refractive index from the double-Debye relaxation model. In Fig. 7(b), we compare the absorption coefficient in this work with that from the double-Debye relaxation model obtained at a room temperature. We found a close match to the double-Debye model, however, a slight variation in the higher frequency range is seen. Since the Debye model is obtained at room temperature, heat generated by the spinning wheel results in slight discrepancies in the absorption coefficient.

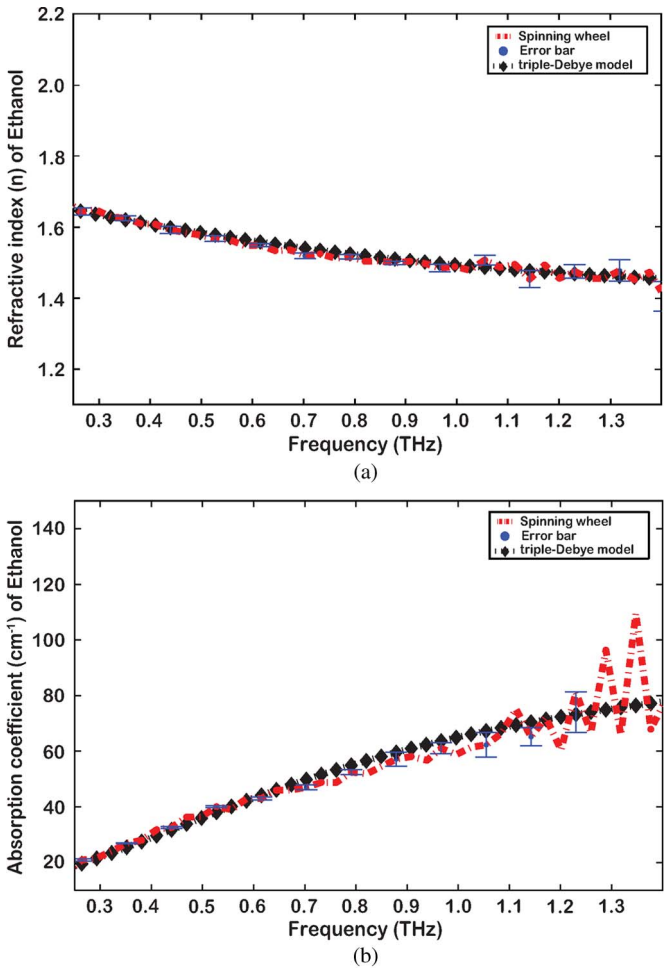

Fig. 9. The absorption coefficient and refractive index of ethanol. This figure illustrates the measured terahertz dielectric properties of ethanol. The measured data is compared with the triple-Debye relaxation model. A close match is demonstrated. The estimated uncertainty in the calculated values is indicated by the error bars.

4.2. Methanol

Methanol is flammable polar liquid and its dielectric properties are well explored in terahertz regime [4], [12]–[14]. Here, the dielectric properties of methanol are measured using the double-modulated dual-thickness spinning wheel technique. Fig. 8 shows the terahertz dielectric properties of methanol. Fig. 8(a) compares the measured refractive index with refractive index obtained from the triple-Debye relaxation model. The results are in an excellent agreement with the triple-Debye relaxation model. In Fig. 8(b), an excellent match between the measured absorption coefficient and the absorption coefficient obtained from triple-Debye model is demonstrated.

4.3. Ethanol

Ethanol is another flammable polar liquid, which has drawn an attention among terahertz researchers. The dielectric properties of ethanol are well explored in terahertz regime [3], [4] as well as in the gigahertz regime [14], [15]. In this section, we demonstrate the measurement results of the double-modulated dual-thickness technique, which is then compared with the triple-Debye relaxation model. The fitting parameters for the triple-Debye model are obtained from [4]. According to our observation in Fig. 9(a), the measured refractive index of ethanol matches well with refractive index derived from the triple-Debye model. In Fig. 9(b), the absorption coefficient of ethanol is

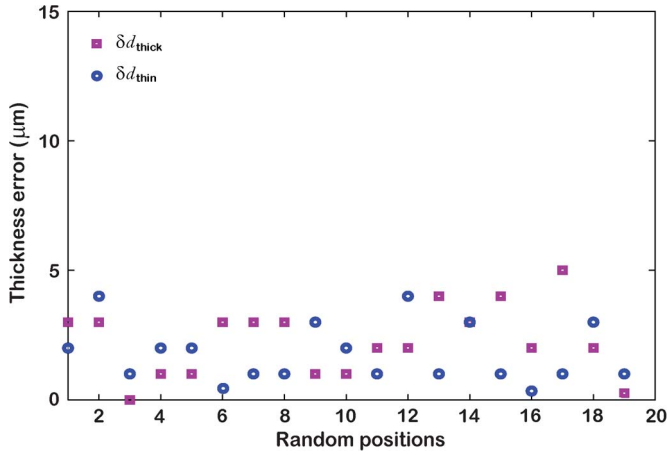

Fig. 10. Sample thickness error present at random positions in the thin and thick liquid layer of the fixed dual-thickness liquid sample holder. This plot shows that the δd for thin and thick liquid layer is less than 5 μm.

compared with absorption coefficient calculated from triple-Debye model. Here, a close match is demonstrated.

Fig. 10, shows the sample thickness error present in the thin and thick liquid layers of the fixed dual-thickness liquid sample holder. Based on the graph, one can say that δd_{thin} and δd_{thick} are less than 5 μm, as compared to 100 μm in the previously presented dithering technique [9].

5. Conclusion

An approach for obtaining terahertz dielectric properties of thin-layered liquids using a spinning wheel technique is demonstrated. We have shown an improvement in the dual-thickness geometry by introducing a fixed dual-thickness window cell using COC 5013L10 polymer material. The 100-μm sample thickness error introduced by linear dithering is reduced to less than 5 μm with our implementation of a fixed dual-thickness geometry. This work also highlights that bubble-free liquid measurement is achievable with a spinning wheel technique. Moreover, a rapid succession measurement between reference and sample signals is demonstrated. The measurement results show a good agreement with the Debye relaxation model. Therefore, this demonstrates the accuracy of the dual-thickness spinning wheel technique.

Appendix

The output detected at LIA1 (Mean) and LIA2 (Amplitude) is used to extract the frequency-dependent reference and sample signals based on the following formulas [9]:

$$\widetilde{E}_{\text{ref}}(\omega) = \widetilde{E}_{\text{mean}}(\omega) + \widetilde{E}_{\text{amplitude}}(\omega) \tag{1}$$

$$\widetilde{E}_{\text{sam}}(\omega) = \widetilde{E}_{\text{mean}}(\omega) - \widetilde{E}_{\text{amplitude}}(\omega). \tag{2}$$

Hence, the ratio of $\widetilde{E}_{\text{sam}}$ over $\widetilde{E}_{\text{ref}}$ produces transmission coefficient $T(\omega)$, as shown in following formula:

$$T(\omega) = \frac{\widetilde{E}_{\text{sam}}(\omega)}{\widetilde{E}_{\text{ref}}(\omega)} = \rho e^{-j\phi}. \tag{3}$$

Eq. (3) expands to

$$T(\omega) = \frac{\exp\left(\frac{-j\tilde{n}_3\omega d_{\text{thick}}}{c}\right)}{\exp\left(\frac{-j\tilde{n}_3\omega d_{\text{thin}}}{c}\right) \cdot \exp\left(\frac{-j\tilde{n}_5\omega d_{\text{diff}}}{c}\right)}. \tag{4}$$

Here, $\tilde{n}_3 = n - j\kappa$, $\tilde{n}_5 = 1$, and $d_{\text{diff}} = d_{\text{thick}} - d_{\text{thin}}$. Liquid thicknesses d_{thick} and d_{thin} are set to 170 μm and 20 μm, respectively. By substituting these parameters into Eq. (4), the magnitude ρ and the phase ϕ can be obtained as follows:

$$\rho(\omega) = \exp\left(\frac{-\omega\kappa d_{\text{diff}}}{c}\right) \tag{5}$$

$$\phi(\omega) = \frac{\omega d_{\text{diff}}(n(\omega) - 1)}{c}. \tag{6}$$

Hence, based on the magnitude and phase information from Eqs. (5) and (6), the frequency-dependent refractive index n, extinction coefficient κ, and absorption coefficient α can be deduced as follows:

$$n(\omega) = \frac{\phi(\omega)c_0}{\omega d_{\text{diff}}} + 1 \tag{7}$$

$$\kappa(\omega) = -\frac{c_0}{\omega d_{\text{diff}}}\ln|\rho(\omega)| \tag{8}$$

$$\alpha(\omega) = 2\frac{\kappa(\omega)\omega}{c_0}. \tag{9}$$

1. Spinning Wheel Accuracy Verification

The functionality of the spinning wheel technique for a dual-thickness liquid measurement is experimentally verified using water, ethanol, and methanol. The accuracy of the dielectric properties of the measured water is compared with the double-Debye relaxation model, in which the frequency-dependent complex dielectric constant is given by [16]

$$\hat{\epsilon}(\omega) = \epsilon_\infty + \frac{\Delta\epsilon_1}{1 + i\omega\tau_1} + \frac{\Delta\epsilon_2}{1 + i\omega\tau_2}. \tag{10}$$

The measurement accuracy of the dielectric properties of the measured ethanol and methanol is compared with the triple-Debye relaxation model as follows [16]:

$$\hat{\epsilon}(\omega) = \epsilon_\infty + \frac{\Delta\epsilon_1}{1 + i\omega\tau_1} + \frac{\Delta\epsilon_2}{1 + i\omega\tau_2} + \frac{\Delta\epsilon_3}{1 + i\omega\tau_3}. \tag{11}$$

According to Eqs. (10) and (11), ϵ_∞ is the high-frequency dielectric constant and $\Delta\epsilon_1$, $\Delta\epsilon_2$, and $\Delta\epsilon_3$ refer to relaxation amplitudes. Here, τ_1 is the slow relaxation time constant, and τ_2 and τ_3 are the fast relaxation time constants of liquid. The parameters for the Equations (10) and (11) are obtained from [4]. Since the complex index of refraction is related to the dielectric properties of a material as given in the following equation:

$$\hat{\epsilon}(\omega) = \epsilon'(\omega) - j\epsilon''(\omega) = (n - jk)^2 \tag{12}$$

one can rewrite the above equation in terms of n and α as follows [4]:

$$n(\omega) = \left(\frac{\sqrt{\epsilon'(\omega)^2 + \epsilon''(\omega)^2} + \epsilon'(\omega)}{2} \right)^{\frac{1}{2}} \tag{13}$$

$$\alpha(\omega) = \frac{2\omega}{c} \left(\frac{\sqrt{\epsilon'(\omega)^2 + \epsilon''(\omega)^2} - \epsilon'(\omega)}{2} \right)^{\frac{1}{2}}. \tag{14}$$

Here, $\omega = 2\pi f$, and c is the speed of light.

References

[1] T. Globus, D. Woolard, T. W. Crowe, T. Khromova, B. Gelmont, and J. Hesler, "Terahertz Fourier transform characterization of biological materials in a liquid phase," *J. Phys. D, Appl. Phys.*, vol. 39, no. 15, pp. 3405–3413, Aug. 2006.

[2] T. Ikeda, A. Matsushita, M. Tatsuno, Y. Minami, M. Yamaguchi, K. Yamamoto, M. Tani, and M. Hangyo, "Investigation of inflammable liquids by terahertz spectroscopy," *Appl. Phys. Lett.*, vol. 87, no. 3, pp. 1–3, Jul. 2005.

[3] P. U. Jepsen, U. Mller, and H. Merbold, "Investigation of aqueous alcohol and sugar solutions with reflection terahertz time-domain spectroscopy," *Opt. Express*, vol. 15, no. 22, pp. 14 717–14 737, Oct. 2007.

[4] J. T. Kindt and C. A. Schmuttenmaer, "Far-infrared dielectric properties of polar liquids probed by femtosecond terahertz pulse spectroscopy," *J. Phys. Chem.*, vol. 100, no. 24, pp. 10 373–10 379, Jun. 1996.

[5] J. Pedersen and S. Keiding, "THz time-domain spectroscopy of nonpolar liquids," *IEEE J. Quantum Electron.*, vol. 28, no. 10, pp. 2518–2522, Oct. 1992.

[6] L. Thrane, R. H. Jacobsen, P. U. Jepsen, and S. R. Keiding, "THz reflection spectroscopy of liquid water," *Chem. Phys. Lett.*, vol. 240, no. 4, pp. 330–333, Jun. 1995.

[7] H. Hirori, K. Yamashita, M. Nagai, and K. Tanaka, "Attenuated total reflection spectroscopy in time-domain using terahertz coherent pulses," *Jpn. J. Appl. Phys. 2, Lett.*, vol. 43, no. 10A, pp. L1 287–L1 289, 2004.

[8] L. Cheng, S. Hayashi, A. Dobroiu, C. Otani, K. Kawase, T. Miyazawa, and Y. Ogawa, "Terahertz-wave absorption in liquids measured using the evanescent field of a silicon waveguide," *Appl. Phys. Lett.*, vol. 92, no. 18, art. 181 104, May 2008.

[9] S. P. Mickan, R. Shvartsman, J. Munch, X.-C. Zhang, and D. Abbott, "Low noise laser-based T-ray spectroscopy of liquids using double-modulated differential time-domain spectroscopy," *J. Opt., B Quantum Semiclass. Opt.*, vol. 6, no. 8, pp. S786–S795, Aug. 2004.

[10] J. Balakrishnan, B. M. Fischer, and D. Abbott, "Spinning wheel technique for material parameter extraction using double-modulated THz differential time-domain spectroscopy," manuscript in preparation.

[11] J. Balakrishnan, B. M. Fischer, and D. Abbott, "Sensing the hygroscopicity of polymer and copolymer materials using terahertz time-domain spectroscopy (THz-TDS)," *Appl. Opt.*, vol. 48, no. 12, pp. 2262–2266, Apr. 2009.

[12] D. S. Venables and C. A. Schmuttenmaer, "Spectroscopy and dynamics of mixtures of water with acetone, acetonitrile, and methanol," *J. Chem. Phys.*, vol. 113, no. 24, pp. 11 222–11 236, Dec. 2000.

[13] M. Asaki, A. Redondo, T. Zawodzinski, and A. Taylor, "Dielectric relaxation of electrolyte solutions using terahertz transmission spectroscopy," *J. Chem. Phys.*, vol. 116, no. 19, pp. 8469–8482, May 2002.

[14] T. Sato and R. Buchner, "Cooperative and molecular dynamics of alcohol/water mixtures: The view of dielectric spectroscopy," *J. Mol. Liq.*, vol. 117, no. 1–3, pp. 23–31, Mar. 2005.

[15] P. Petong, R. Pottel, and U. Kaatze, "Water-ethanol mixtures at different compositions and temperatures. A dielectric relaxation study," *J. Phys. Chem., A*, vol. 104, no. 32, pp. 7420–7428, Aug. 2000.

[16] P. Debye, "Reaction rates in ionic solutions," *Trans. Electrochem. Soc.*, vol. 82, no. 1, pp. 265–271, Oct. 1942.